IEEE Access
Multidisciplinary | Rapid Review | Open Access Journal

Received 17 June 2022, accepted 7 July 2022, date of publication 13 July 2022, date of current version 18 July 2022.

Digital Object Identifier 10.1109/ACCESS.2022.3190544

RESEARCH ARTICLE

Phase Estimation of Single Tones Next to Modulated Signals in the Medium Frequency R-Mode System

LARS GRUNDHÖFER[1], (Graduate Student Member, IEEE), MARKUS WIRSING[1], STEFAN GEWIES[1], AND GIOVANNI DEL GALDO[2,3], (Member, IEEE)

[1]German Aerospace Center, Institute of Communications and Navigation, 17235 Neustrelitz, Germany
[2]Institute for Information Technology, Technische Universität Ilmenau, 98693 Ilmenau, Germany
[3]Fraunhofer Institute for Integrated Circuits IIS, 98693 Ilmenau, Germany

Corresponding author: Lars Grundhöfer (lars.grundhoefer@dlr.de)

This work was supported by the European Union through the European Regional Development Fund within the Interreg Baltic Sea Region Program under Project R-Mode Baltic 2.

ABSTRACT Position, navigation, and timing information are critical to today's infrastructures; as a result, the possibility of estimating ranges is being explored in more and more radio systems. One way to achieve this is to extend the modulation with time-synchronised aiding carriers and to estimate their phase at the receiver side. In this paper, we present two ways to minimise the negative influence of the modulation on the phase estimation. We show that the classical maximum likelihood estimator is still an efficient estimator for our problem, using a medium-frequency R-Mode signal as an example, and is therefore used in receiver designs. We then describe two possible ways to precondition the signal to increase the accuracy for short observations. As a first approach, we describe how window functions can positively change the signal-to-noise ratio for our estimation. As a second approach, we show the use of a narrowband bandpass filter. Finally, we show that these approaches, applied to real measurements, improve the variance of the estimate by up to two orders of magnitude.

INDEX TERMS APNT, R-Mode, phase estimation, navigation, signal processing.

I. INTRODUCTION

Position, navigation and timing (PNT) information is critical to today's industrial, commercial and transportation infrastructure. The primary source of PNT information today is global navigation satellite systems (GNSS), but GNSS has been found to be vulnerable to jamming and spoofing, whether intentional or unintentional [1], [2]. This leads to problems for the maritime user in particular [3], [4]. Therefore, alternative systems are needed and discussions are underway to modify existing radio systems to provide PNT capabilities. An approach for Frequency Division Multiple Access (FDMA) systems is to introduce unmodulated auxiliary transmissions, often referred to as continuous waves, into the zero crossing in the spectra of the modulation [5]. When the signals from different stations are synchronised with each other, we can then derive PNT information from the phase-estimation of these aiding carriers. One system in which this approach is implemented is the medium-frequency R-Mode, a terrestrial navigation system in the frequency band from 283.5 kHz to 315.0 kHz [6]. The system is based on the parameter estimation of harmonics, which has been a well-investigated research area in the field of signal processing. Estimating, e.g. the directions of arrival, frequencies, Doppler shifts, phase and more is required in a wide range of applications including radar [7], sonar [8], channel sounding [9], wireless communications [10] and power electronics [11]. Therefore, different methods can be used to estimate the harmonics parameter such as the discrete Fourier transform (DFT) [12], [13], phase lock loop [14] and more recent techniques such as ESPRIT [15] and MUSIC [16]. We had shown that the modulated signal affects the accuracy of the

The associate editor coordinating the review of this manuscript and approving it for publication was Kegen Yu.

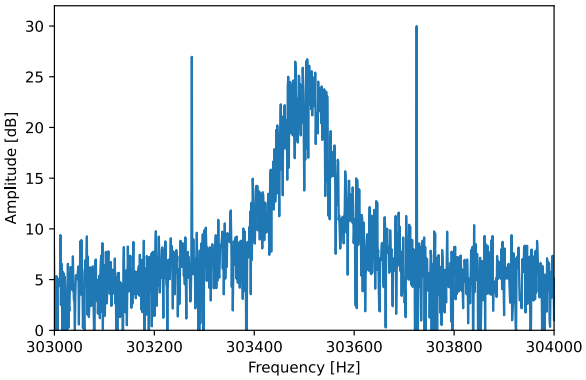

FIGURE 1. Simulated spectrum of R-Mode signal with centre frequency 303.5 kHz.

phase-estimation of the aiding carriers when the DFT is used as maximum likelihood estimator. We assume, that this is due to the fact that the assumption of white Gaussian noise is not valid any more [17], [18]. However, this estimator is of practical relevance, as it can be implemented in a highly computational effective way [13] to estimate multiple harmonics. In this work, we investigate the influence of the modulated signal on the parametric estimation of a nearby single tone and propose a preconditioning of the signal. The overall goal is to match the Gaussian condition as close as possible, to derive the best results without deriving new estimation techniques. To verify our results, we use medium-frequency R-Mode as an example application and show how the performance can be improved.

The paper starts with a short description of the signal in Section II. We show in section III that the recently used maximum likelihood estimator [19] is an efficient estimator for our problem. In Section IV, we further investigate how we can improve the estimator with windowing for short observation times. In Section V, we present an alternative to the windowing approach by using a narrow bandpass-filter. The improved performance is demonstrated using real measurements in Section VI.

II. SIGNAL DESCRIPTION

We use the medium-frequency R-Mode signal as an example of an alternative PNT signal that uses continuous waves. The legacy signal consists of a Minimum Shift Keyed (MSK) modulation scheme [20] containing the messages specified by the Radio Technical Commission for Maritime Services (RTCM) [21]. Typical data rates are 100 bit/s with a channel bandwidth of 500 Hz in Europe.

To utilise the legacy signal for R-Mode, two single tones with an offset of ±225 Hz to the carrier frequency of the transmitter are introduced [6]. We call the lower carrier CW1 (continuous wave one) and the upper carrier CW2 (continuous wave two). Because of the relatively short wavelength with respect to the distance to estimate, we have to solve ambiguities. This is carried out by calculating the beat frequency of CW1 and CW2, which gives a signal of 450 Hz with a wavelength of 666 km which is larger than the range of a transmitter.

To provide an example of how the signal looks in a single channel, we simulated the signal with our Python simulation environment, which is also used for all other simulations in this paper. We plot a spectrum of the simulated signal at a centre frequency of 303.5 kHz in Fig. 1. These signals are already available in the R-Mode Baltic testbed [22] and were used for initial positioning in the Baltic Sea, using the Fast Fourier Transform (FFT) as the maximum likelihood estimator for the different phases [19].

III. EFFICIENT ESTIMATOR

In our previous publication [18], we had shown that we can assume the Cramér-Rao lower bound (CRB) for the estimation of the phase $\hat{\theta}_n$ of the n-th subcarrier, in the absence of a modulated signal, to be

$$\mathrm{var}(\hat{\theta}_n) \geq \frac{2\sigma^2}{N A_n^2} \tag{1}$$

and for the beat phase $\hat{\theta}_{\mathrm{beat}}$ between the two tones to be

$$\mathrm{var}(\hat{\theta}_{\mathrm{beat}}) \geq \frac{2\sigma^2(A_1^2 + A_2^2)}{N A_1^2 A_2^2}, \tag{2}$$

where A_n is the amplitude of the signal, σ^2 is the variance of the noise and N is the number of samples evaluated. Since (2) is the sum of the variances of the two continuous waves, our estimates must be statistically independent. However, it has been shown that we generally cannot achieve the bound for short observation times because of the modulated signal interfering. Since we use an FFT as a maximum likelihood estimator [14], the considered bandwidth is reduced for longer observation times and thus the power leakage of the modulated signal is decreased. Therefore, for long observation times, we expect to reduce the influence of the modulation and achieve the CRB.

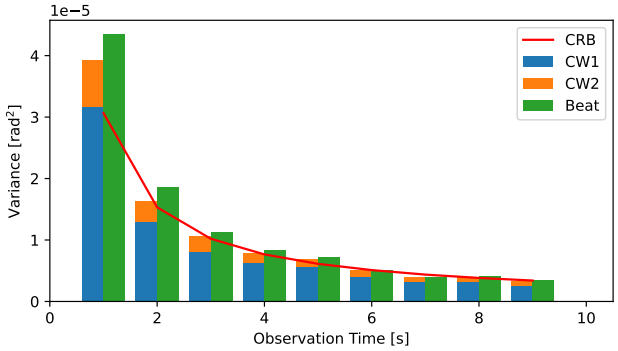

FIGURE 2. Cramér-Rao bound compared to simulation result for different observation times.

To test this hypothesis, we performed a Monte-Carlo simulation with 500 runs at a noise variance of 1.22×10^{-5} for different observation times T_{obs} increased by integer steps. We chose the amplitudes $A_1 = 0.001$, $A_2 = 0.002$ for the

CW carriers and $A_{\mathrm{MSK}} = 0.004$ for the modulated MSK signal. A_1 and A_2 were chosen differently to reflect possible imperfections of the R-Mode signals. In general, the amplitudes match our observation in the testbed [19]. The results of this comparison are shown in Fig. 2. Here, the variance of the obtained phase is shown as a blue bar for CW1, an orange bar for CW2 and a green bar for the beat signal for increasing length of observation time. Moreover, the Cramér-Rao bound for the beat signal is shown as a red line. We can clearly see that the simulations do not reach the bound for the shorter observation time. With longer observation time, however, we see a good agreement between the estimate and the bound. In some places, our estimator even seems to outperform the bound, which is due to the limited number of simulation runs. Therefore, our assumption that the influence of the MSK signal component is smaller with longer observation times seems to hold and the maximum likelihood estimator [14] behaves like an efficient estimator for our problem.

IV. WINDOWING

Extending the observation time to achieve the best performance is not always possible. However, the current R-Mode receiver implementation relies on the fast Fourier transform [19] as an estimator, due to its computational efficiency. To further improve this suboptimal approach while retaining its benefit of computational efficiency, we suggest using windowing to decrease the variance for short observation times. It has been shown that we cannot achieve the CRB if we use windowing [23] when only white noise is assumed, but we can attenuate the power leakage of the modulated signal and thus improve the performance of our estimator.

In order to have a parametrised window that can be customised, we use the modified Hann window defined as follows [24]:

$$w_{\mathrm{hann}}(t) = \left[a_0 - (1-a_0)\cos\left(\frac{2\pi t}{T_{\mathrm{obs}}}\right)\right]\mathrm{rect}\left(\frac{t}{T_{\mathrm{obs}}}\right), \quad (3)$$

which depends on the design parameter a_0 and the observation time T_{obs}. We choose the window due to the dependencies on only one parameter, which we can easily adjust in our application. Furthermore, we obtain a rectangular window for the case $a_0 = 1$. Therefore we can continuously observe the influence of the sidelobe suppression.

Since a Monte Carlo simulation would take too long to adaptively adjust the window for real applications, we are interested in finding a performance metric that allows us to assess a window performance under given conditions. Here, our main idea is to compare the noise and signal energies for the bin of interest that are collected from different windows. Therefore, we will show that the signal-to-noise ratio (SNR) can be used as a figure of merit. This can be described analytically by considering the Fourier transform of a signal $s(t)$ that is observed for a duration of T_{obs}:

$$S_{\mathrm{obs}}(f) = \int_{-\frac{T_{\mathrm{obs}}}{2}}^{\frac{T_{\mathrm{obs}}}{2}} s(t) e^{2\pi jft}\, dt, \quad (4)$$

where, without loss of generality, we centre the observation window at $t = 0$. S_{obs} denotes the spectrum of the observed part of the signal.

If we assume a window $w(t)$, we can express the time limit with the function, which leads to the following expression:

$$S_{\mathrm{obs}}(f) = \int_{-\infty}^{\infty} s(t) w(t)\, e^{2\pi jft}\, dt. \quad (5)$$

For our estimation problem, we are interested in $S(f_c)$, which is the value of the Fourier transform at the specific frequency f_c where the CW carrier is located.

We apply Parseval formula [25] which leads to

$$S_{\mathrm{obs}}(f_c) = \int_{-\infty}^{\infty} S(f) W(f - f_c) df. \quad (6)$$

Here, $S(f)$ corresponds to $s(t)$ and $W(f)$ to $w(t)$ as a time-continuous Fourier transform. This is the evaluation of a single point in the convolution operation between the signal spectrum and the window spectrum.

We can define our signal $s(t)$ with the continuous waves $s_{\mathrm{CW}}(t)$, the MSK modulation $s_{\mathrm{MSK}}(t)$ and the noise term $n(t)$ as

$$s(t) = s_{\mathrm{CW}}(t) + s_{\mathrm{MSK}}(t) + n(t). \quad (7)$$

Thus, S_{obs} can also be expressed in terms of the Fourier transforms of these parts:

$$S_{\mathrm{obs}}(f_c) = \int_{-\infty}^{\infty} (S_{\mathrm{CW}}(f) + S_{\mathrm{MSK}}(f) + N(f)) W(f - f_c) df \quad (8)$$

$$= \int_{-\infty}^{\infty} S_{\mathrm{CW}}(f) W(f - f_c) df \quad (9)$$

$$+ \int_{-\infty}^{\infty} (S_{\mathrm{MSK}}(f) + N(f)) W(f - f_c) df, \quad (10)$$

where (9) represents the desired part of (8), and (10) the undesired part that is caused by noise and the interfering MSK signal.

Our goal is to maximise the contribution of (9) and to minimise the contribution of (10). We thus consider the quotient of the energies contributed by each component:

$$\mathrm{SNR} = \frac{\left(\int_{-\infty}^{\infty} S_{\mathrm{CW}}(f) W(f - f_c) df\right)^2}{\left(\int_{-\infty}^{\infty} (S_{\mathrm{MSK}}(f) + N(f)) W(f - f_c) df\right)^2} \quad (11)$$

To find an optimal window for our problem, we need to find the window parameter a_0 for which (11) is maximised. This represents a compromise between the process gain, the peak sidelobe level and the equivalent noise bandwidth. Each of these values represents a different influence on the frequency range we want to estimate. Here, the process gain describes the reduced power of our signal when a window is applied, while the peak sidelobe level indicates the largest sidelobe and can therefore be an indicator of how well the modulation, a near-band signal, is suppressed. The contribution of the noise floor is also described by the equivalent noise bandwidth, which equals the width of a rectangular window with

the same peak power gain that would produce the same noise power [24].

With this parameter we can influence the noise contribution in the near and broadband range as well as the signal power and thus the SNR. We have visualised the basic concept in Fig. 3, where we see the Fourier transform of two different window functions, namely a rectangular and a Hann window with $a_0 = 0.5$. The Hann window has a wider main lobe, but suppresses energy further away, while the rectangular window has a lower noise suppression and a smaller side lobe.

It becomes clear that the design parameters of the window optimise the SNR for a given noise floor. We evaluate the SNR for different parameters a_0 to iteratively approach the optimal solution.

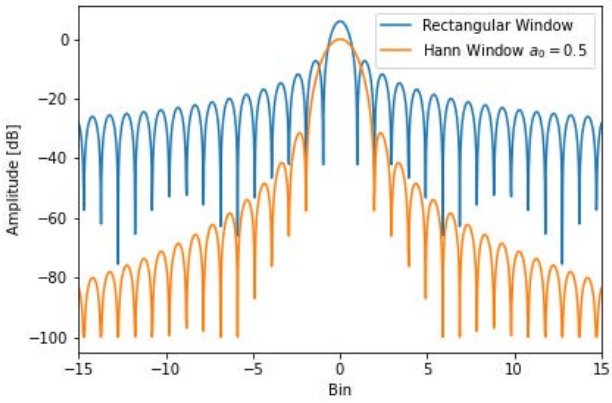

FIGURE 3. Fourier transform of Hann and rectangular window functions.

A. WINDOWING IN ESTIMATION

To verify the obtained result, we performed a Monte Carlo simulation with 5000 runs and an observation interval of 1 s to investigate the problem in detail and compare the results with our assumptions. We chose the amplitudes for CW1 to be $A_1 = 0.001$, for CW2 to be $A_2 = 0.002$ and for the MSK signal to be $A_{\mathrm{MSK}} = 0.004$. We used as reference a case with no window and six different modified Hann windows with $a_0 = [0.4, 0.5, 0.54, 0.6, 0.7, 0.8]$ in three different noise conditions, which are generated by linear scaling the amplitude of a generated white-noise process. It is important to note that the window for $a_0 = 0.54$ is called the Hamming window and has the greatest suppression of the first side lobe [24].

We show the results of this simulation as a bar graph of the phase-estimation variance, where a noise variance of 2.50×10^{-7} is further denoted as low noise in Fig. 4, a noise variance of 1.22×10^{-5} denotes medium noise in Fig. 5 and the highest noise variance of 8.09×10^{-5} in Fig. 6 is further referred to as high noise. In all three figures, the blue bar shows the results for CW1, the orange bar for CW2 and the green bar for the beat signal. In addition, the red solid line shows the theoretical CRB for the beat variance and the

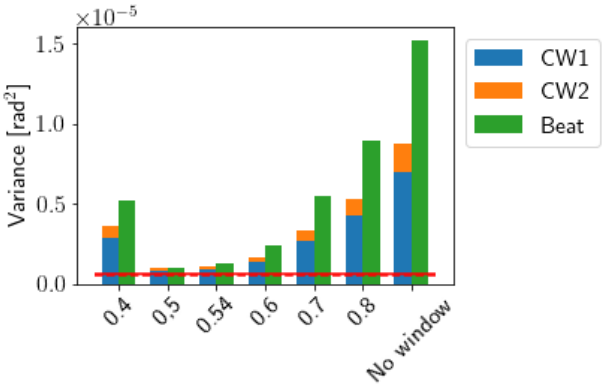

FIGURE 4. Bar graph for the resulting phase estimate variance with varying window parameters under low noise conditions.

dashed line indicates the lower limit of CW1 for the simulated noise level.

For the low-noise case in Fig. 4, we can clearly see that the estimation without window is far from the optimal performance and our result improves when we lower the parameter a_0. The minimum is reached at the test point for $a_0 = 0.5$, where we are close to the lower bound. After that, the variance starts to increase again. We would like to emphasise that also the variance of the beat estimate is close to the sum of CW1 and CW2, when we use $a_0 = 0.5$ as parameter. This is what we expect as long as the MSK interference is a leading contributor to the total variance, since we have attenuated the signal correlating with the tone. We also see that the maximum suppression of the first sidelobe is achieved for parameter $a_0 = 0.4$, does not give the best result. This is due to the fact that the MSK signal is already largely suppressed, so that disturbances further away have a greater influence and decrease the performance.

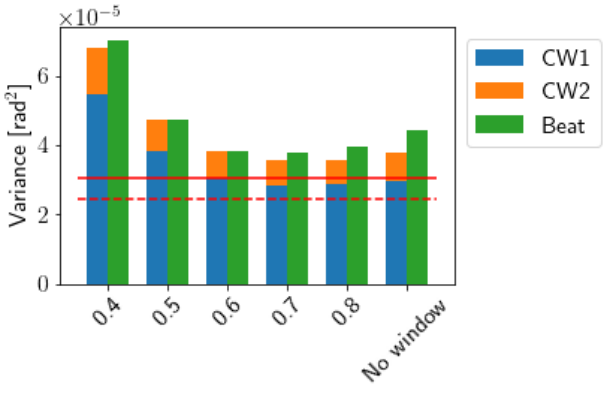

FIGURE 5. Bar graph for the resulting phase estimate variance with varying window parameters under medium noise conditions.

In Fig. 5, we can see that for smaller values of a_0, we obtain larger variance values. However, we can optimise the estimation result by applying a window with $a_0 = 0.7$. We therefore

became aware that we need a different compromise between MSK and broadband noise suppression than before.

In the presence of strong noise, as per the result in Fig. 6, the non-windowed case slightly outperforms the window with $a_0 = 0.8$. It becomes clear that the influence of the noise is the main influence, and we obtain too much broadband noise if we try to suppress the modulated signal.

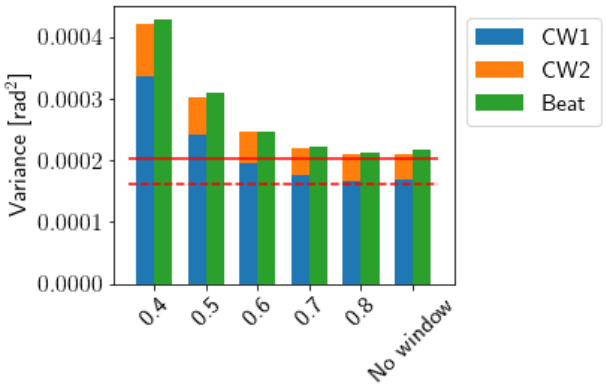

FIGURE 6. Bar graph for the resulting phase estimate variance with varying window parameters under high noise conditions.

We have used the SNR as a figure of merit, to find the best parameter a_0. To determine the SNR, we perform an FFT on the simulated signal on which we applied the window, without the carrier we are interested in, in order to obtain the noise energy in the range we are looking at. We then apply the FFT to the carrier only, again applying the window, to obtain the signal power we need to consider. This is performed in a separate Python script that allows us to find an optimal window for a given noise and signal power. This gives us a clear SNR value that we can compare with the performance of each window.

In Tab. 1, we compare the SNR results for the three noise levels with the variance of the phase estimate from the Monte Carlo simulation, both for CW1. We can clearly see that the window affects the SNR, and in most cases we obtain a lower variance for higher SNR values, which is expected and can be seen in (1) when we consider SNR $= A_n^2/\sigma^2$. We notice that the SNR at high-noise is slightly higher for the non-window than for the better-performing window $a_0 = 0.8$. We observe a similar behaviour for the medium-noise case, and the parameter at $a_0 = 0.7$ and $a_0 = 0.8$. This is a simulation issue due to the limited simulation time and lies within the expected accuracy of this configuration. The improvement resulting from this step is only minor. Therefore, it is clear that the resulting SNR is a good metric for optimising our window to estimate the phase near a modulation. Overall, we see a good agreement between our assumptions and the simulated results.

V. PREFILTERING

From the windowing approach presented in the previous section, it is clear that we need to find a compromise between

TABLE 1. Window comparison results for CW1 phase-estimation.

Noise level	Parameter	SNR	var(CW1)
Low	$a_0 = 0.4$	483.19	2.89×10^{-6}
	$a_0 = 0.5$	949.55	8.12×10^{-7}
	$a_0 = 0.54$	921.00	8.94×10^{-7}
	$a_0 = 0.6$	720.06	1.35×10^{-6}
	$a_0 = 0.7$	514.15	2.67×10^{-6}
	$a_0 = 0.8$	417.56	4.24×10^{-6}
	no window	328.32	6.99×10^{-6}
Medium	$a_0 = 0.4$	106.60	5.45×10^{-5}
	$a_0 = 0.5$	132.43	3.83×10^{-5}
	$a_0 = 0.54$	139.71	3.37×10^{-5}
	$a_0 = 0.6$	147.59	3.07×10^{-5}
	$a_0 = 0.7$	153.91	2.83×10^{-5}
	$a_0 = 0.8$	154.41	2.88×10^{-5}
	no window	148.61	2.98×10^{-5}
High	$a_0 = 0.4$	42.21	3.38×10^{-4}
	$a_0 = 0.5$	50.36	2.42×10^{-4}
	$a_0 = 0.54$	52.87	2.18×10^{-4}
	$a_0 = 0.6$	55.86	1.97×10^{-4}
	$a_0 = 0.7$	58.99	1.77×10^{-4}
	$a_0 = 0.8$	60.41	1.67×10^{-4}
	no window	60.73	1.68×10^{-4}

narrowband and broadband noise suppression. In this section, we want to investigate whether we can suppress the noise by applying a narrowband filter to each signal to be estimated. This would increase the processing power considerably, as we have to implement a filter and an estimation for each signal of interest.

In order to design a narrow bandpass filter, we choose to mitigate the tone of interest by a Notch filter. The resulting samples are then subtracted from the original signal, as presented in Fig. 7. In this way we only need to adjust the frequency we want to cancel out with the Notch filter, instead of adjusting the whole passband. We begin by designing a notch filter that matches the tone of interest with the response function [26]

$$H(z) = \frac{1 - z_0\, z^{-1}}{1 - k\, z_0\, z^{-1}} \text{ with } 0 \leq k < 1, \tag{12}$$

where z_0 is the complex zero point, which represents the frequency to be suppressed and which can be calculated via the frequency according to

$$z_0 = e^{j\,2\,\pi\, f_0\, T_{\text{obs}}}. \tag{13}$$

Here, f_0 is the frequency to be cancelled in Hertz and T_{obs} the sampling interval in seconds. The position of the pole depends on k, the so-called contraction factor. It is important to note that the width of the filter depends on this parameter [27].

To apply the maximum likelihood estimation we, first need to apply the pre-filtering, then split the sample into subsets and estimate the phase of each one. We then subtract the filtered set from the original set, in order to obtain a signal that consists only of the signal of interest, as described in Fig. 7.

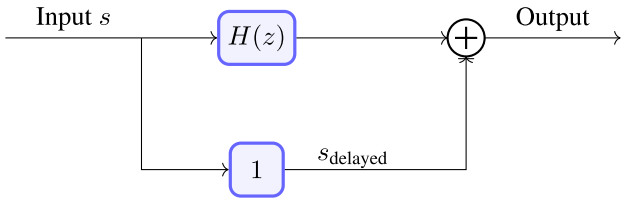

FIGURE 7. Block diagram of notch filter.

On the filtered signal, we apply the maximum likelihood estimation. Since the filter introduces a phase shift, which results in a shifted phase in the estimate, our result is now biased, as we do not apply forward-backward filtering. Here, we only evaluate the variance, therefore any existing bias is not taken into account. For R-Mode as an application, this can be neglected, since the bias caused by different effects is determined after the phase estimation. The overall bias of DSP and hardware delays will be estimated during the receiver calibration and subtracted for ranging [19].

To verify this approach, we perform a Monte Carlo simulation with the same parameters as in the previous section. For the notch filter, we choose a contraction factor of $k = 0.9999$ and obtain the results shown in Figs. 8, 9 and 10 with the most appropriate window approach for the noise level. In these figures, we again use the same colour scheme as previously described for Fig. 4.

In Fig. 8, the prefiltering approach exceeds the window with $a_0 = 0.5$ for the low-noise case and comes close to the CRB with a variance of 5.52×10^{-7} rad^2 for CW1. For the case of medium noise, for which we show the results in Fig. 9, we need to compare the performance with a window with $a_0 = 0.7$. Here, the window approach performs slightly better than the notch approach, while neither technique comes close to the CRB.

In the last scenario, with high-noise, in Fig. 10, we see again that the notch filter performs worse than our window approach for the single CW estimates. This changes for the beat estimation, where the notch approach performs slightly better. Again, the resulting estimates have quite a large gap from the CRB. However, the notch filters show good suppression of the correlation introduced by the MSK modulation, so that we achieve nearly statistically independent results. In addition, we find that the notch filter shows an improvement across all noise levels, whereas the different windows only show an improvement in a certain range.

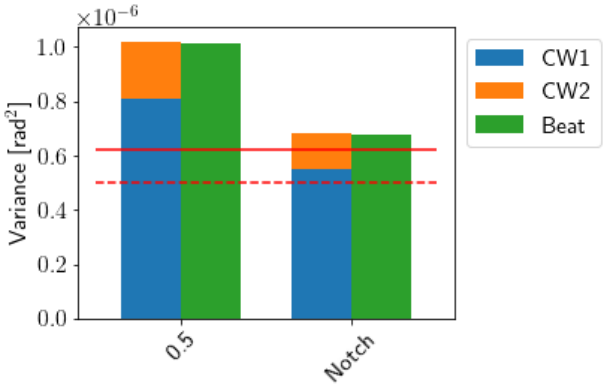

FIGURE 8. Bar plot for different window parameters in low noise conditions.

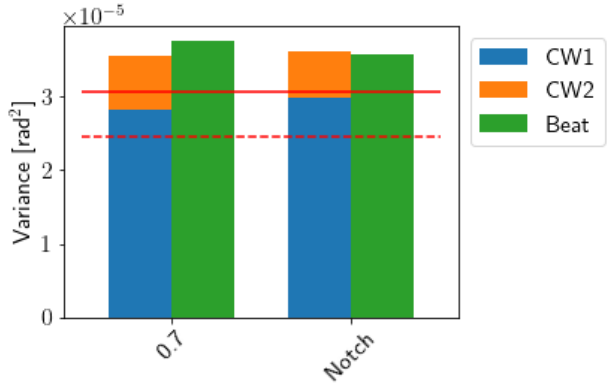

FIGURE 9. Bar plot for different window parameters in medium noise conditions.

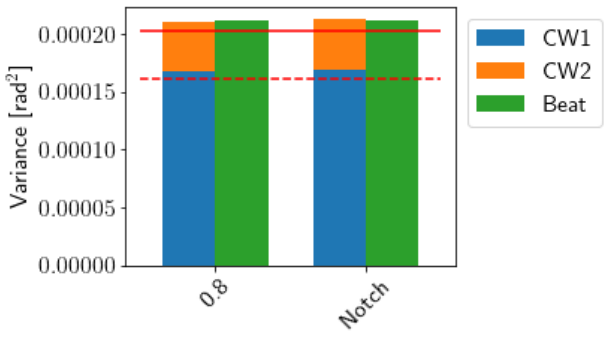

FIGURE 10. Bar plot for different window parameters in high noise conditions.

VI. REAL-WORLD TEST

In the simulation performed, the interference environment was simplified to one channel and white Gaussian noise. In reality, we also have to consider other nearby R-Mode transmitters or other distortions. To provide a real-world example that can be compared with our simulation, we performed measurements in the near-field of the Zeven transmitter in June 2020. Due to the strong signal in the near-field of the station, inter-channel interference is expected to be the major contributor and a high SNR is expected. This setup was designed as a technical demonstration of system-time synchronisation between different stations [28]. Therefore, we only consider the first 5 min of observation in every hour in this paper, which should be sufficient to show short-term influences due to the modulation.

For this measurement, we use the hardware of the medium-frequency R-Mode receiver of the German Aerospace Center,

which consists of an SDR, a bandpass filter and an E-field antenna, as described in more detail in [19].

The preconditioning of our signal improves the variance of our estimate of the nearby station considerably, so that a graphical comparison is no longer possible. Instead, we present the results in Tab. 2, where we list the results for the window parameters $a_0 = 0.5$ and $a_0 = 0.8$, the notch filter approach and the estimation without preconditioning. We can clearly see that the window cases outperform the other test cases by two orders of magnitude. On the other hand, the notch filter also outperforms the non-windowed case. The windowed case $a_0 = 0.5$ shows the best performance, which is to be expected based on our simulation. Since the beat variance is lower than the sum of the carrier estimates, this suggests that there is another general disturbance that can be suppressed by the window but not by our narrow bandpass filter, which potentially describes the divergence from our simulation. In the future, the actual noise floor needs to be investigated in more detail.

TABLE 2. Comparison results for real-world phase-estimation variance in rad^2 of Zeven Station.

Parameter	var(CW1)	var(CW2)	var(Beat)
$a_0 = 0.5$	1.30×10^{-6}	2.24×10^{-6}	1.20×10^{-6}
$a_0 = 0.8$	6.55×10^{-6}	3.64×10^{-6}	1.29×10^{-5}
Notch	0.0041	0.0116	0.0298
No window	0.0059	0.0440	0.0177

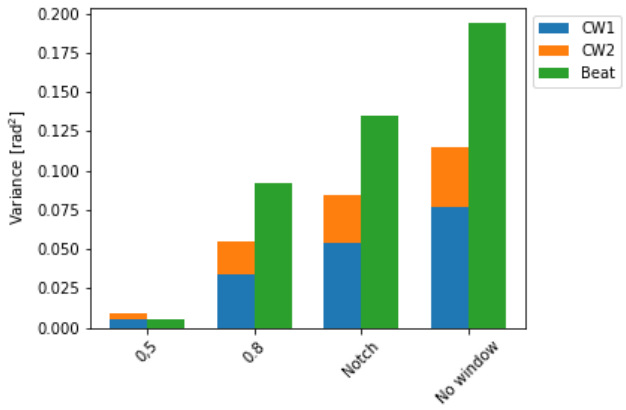

FIGURE 11. Bar plot with different applied signal-preconditioning approaches for the Heligoland signal received in Zeven.

In addition, with such a strong signal, all close channels benefit from near-band rejection, as described in section IV. Therefore, in our measurements we evaluate the signal from the Heligoland station, with a band-gap of 5 kHz and a distance of 134 km to the local station, which can potentially be used for synchronisation. We evaluate the recorded signal for the Heligoland station signal, presenting the results in Fig. 11. Here, we show the resulting variance for CW1 in blue, for CW2 in orange and for the beat signal in green again. Since we now have coloured noise, we do not show the CRB in this plot. Similar to the local signal, the notch filter performs better than the non-window filter. Again, the windowed approach, where $a_0 = 0.5$ outperforms all tested approaches by almost an order of magnitude.

VII. CONCLUSION

In this paper we have analysed ways to improve the accuracy of phase estimation for unmodulated carriers alongside a modulated signal when the observation time is short.

We indicated that the well-known maximum likelihood estimator for the parameter estimation of a signal is an efficient estimator, even in the presence of a modulated signal.

However, for a given observation time, the resulting performance can be improved by applying a parameterised Hann window. We were able to show that maximising the SNR is a good approach for finding the optimum window parameter. Furthermore, we determined that a narrow bandpass filter can also increase the accuracy under good noise conditions, but would require significantly more computational power.

In addition, we have proven that signal conditioning improves performance in close proximity to a station with real measurements and therefore can improve the R-Mode time synchronisation between different stations.

For the future, we would need to implement adaptive preconditioning for the German Aerospace Center R-Mode receiver in the mid-frequency range. The application of the derived techniques will improve the overall performance of the phase-estimation near a modulated signal as used in the R-Mode, if the current noise floor is properly taken into account.

REFERENCES

[1] A. Jafarnia-Jahromi, A. Broumandan, J. Nielsen, and G. Lachapelle, "GPS vulnerability to spoofing threats and a review of antispoofing techniques," *Int. J. Navigat. Observ.*, vol. 2012, Jul. 2012, Art. no. 127072.

[2] M. G. Amin, P. Closas, A. Broumandan, and J. L. Volakis, "Vulnerabilities, threats, and authentication in satellite-based navigation systems [scanning the issue]," *Proc. IEEE*, vol. 104, no. 6, pp. 1169–1173, Jun. 2016.

[3] D. Medina, C. Lass, E. P. Marcos, R. Ziebold, P. Closas, and J. García, "On GNSS jamming threat from the maritime navigation perspective," in *Proc. 22nd Int. Conf. Inf. Fusion (FUSION)*, 2019, pp. 1–7.

[4] E. P. Marcos, S. Caizzone, A. Konovaltsev, M. Cuntz, W. Elmarissi, K. Yinusa, and M. Meurer, "Interference awareness and characterization for GNSS maritime applications," in *Proc. IEEE/ION Position, Location Navigat. Symp. (PLANS)*, Apr. 2018, pp. 908–919.

[5] P. Swaszek, "Analysis of MF-DGNSS modifications for improved ranging," in *Proc. Eur. Navigat. Conf. (ENC)*, 2014, pp. 1–15.

[6] G. Johnson and P. Swaszek, "Feasibility study of R-mode using MF DGPS transmissions," ACCSEAS, Tech. Rep., 2014. [Online]. Available: https://www.iala-aism.org/content/uploads/2016/08/accseas_r_mode_feasibility_study_mf_dgps_transmissions.pdf

[7] D. Nion and N. D. Sidiropoulos, "Tensor algebra and multidimensional harmonic retrieval in signal processing for MIMO radar," *IEEE Trans. Signal Process.*, vol. 58, no. 11, pp. 5693–5705, Nov. 2010.

[8] H. Cox, "Fundamentals of bistatic active sonar," in *Underwater Acoustic Data Processing* (NATO Advanced Study Institute on Underwater Acoustic Data Processing), Y. T.Chan, Ed. Norwell, MA, USA: Kluwer, 1989.

[9] A. R. M. Haardt and R. S. Thoma, "Multidimensional high-resolution parameter estimation with applications to channel sounding," in *High-Resolution and Robust Signal Processing*. Boca Raton, FL, USA: CRC Press, 2004, pp. 255–338.

[10] M. Pesavento, C. F. Mecklenbräuker, and J. F. Böhme, "Multidimensional rank reduction estimator for parametric MIMO channel models," *EURASIP J. Adv. Signal Process.*, vol. 2004, no. 9, pp. 1–10, Aug. 2004.

[11] M. L. Pay and H. Ahmed, "Parameter estimation of harmonics-polluted single-phase grid voltage signal," *Electr. Eng.*, vol. 102, no. 3, pp. 1351–1359, Feb. 2020.
[12] D. C. Rife and R. R. Boorstyn, "Single tone parameter estimation from discrete-time observations," *IEEE Trans. Inf. Theory*, vol. IT-20, no. 5, pp. 591–598, Sep. 1974.
[13] D. C. Rife and R. R. Boorstyn, "Multiple tone parameter estimation from discrete-time observations," *Bell Syst. Tech. J.*, vol. 55, no. 9, pp. 1389–1410, Nov. 1976.
[14] S. M. Kay, *Fundamentals of Statistical Signal Processing: Estimation Theory*. Upper Saddle River, NJ, USA: Prentice-Hall, 1993.
[15] J. Steinwandt, F. Roemer, M. Haardt, and G. D. Galdo, "Performance analysis of multi-dimensional ESPRIT-type algorithms for arbitrary and strictly non-circular sources with spatial smoothing," *IEEE Trans. Signal Process.*, vol. 65, no. 9, pp. 2262–2276, May 2017.
[16] X. Hu, T. Lyu, M. Zhang, H. Zhang, and T. A. Gulliver, "MUSIC and improved MUSIC algorithms for parameter estimation using a polarization sensitive array," in *Proc. IEEE 21st Int. Conf. Commun. Technol. (ICCT)*, Oct. 2021, pp. 117–126.
[17] L. Grundhöfer and S. Gewies, "R-Mode receiver development for medium frequency signals," *Sci. J. Maritime Univ. Szczecin*, no. 56, pp. 57–62, 2018. [Online]. Available: https://repository.am.szczecin.pl/handle/123456789/2504?show=full
[18] L. Grundhöfer, S. Gewies, and G. D. Galdo, "Estimation bounds of beat signal in the R-mode localization system," *IEEE Access*, vol. 9, pp. 69278–69286, 2021.
[19] L. Grundhöfer, F. G. Rizzi, S. Gewies, M. Hoppe, J. Bäckstedt, M. Dziewicki, and G. D. Galdo, "Positioning with medium frequency R-mode," *Navigation*, vol. 68, no. 4, pp. 829–841, Dec. 2021.
[20] S. Pasupathy, "Minimum shift keying: A spectrally efficient modulation," *IEEE Commun. Mag.*, vol. 17, no. 4, pp. 14–22, Jul. 1979.
[21] *Minimum Performance Standards for Marine eLoran Receiving Equipment, RTCM Special Commitee 127*, Radio Tech. Commission Maritime Services, Alexandria, VA, USA, Jan. 2016.
[22] S. Gewies, A. Dammann, R. Ziebold, J. Bäckstedt, K. Bronk, B. Wereszko, C. Rieck, P. Gustafson, C. G. Eliassen, M. Hoppe, and W. Tycholiz, "R-mode testbed in the Baltic sea," in *Proc. 19th IALA Conf.*, 2018. [Online]. Available: https://elib.dlr.de/120702/
[23] S. Schuster, S. Scheiblhofer, and A. Stelzer, "The influence of windowing on bias and variance of DFT-based frequency and phase estimation," *IEEE Trans. Instrum. Meas.*, vol. 58, no. 6, pp. 1975–1990, Jun. 2009.
[24] F. J. Harris, "On the use of windows for harmonic analysis with the discrete Fourier transform," *Proc. IEEE*, vol. 66, no. 1, pp. 51–83, Jan. 1978.
[25] D. W. Kammler, *A First Course in Fourier Analysis*. Cambridge, U.K.: Cambridge Univ. Press, 2008.
[26] D. Borio, "Loop analysis of adaptive notch filters," *IET Signal Process.*, vol. 10, no. 6, pp. 659–669, 2016.
[27] W. Qin, F. Dovis, M. T. Gamba, and E. Falletti, "A comparison of optimized mitigation techniques for swept-frequency jammers," in *Proc. Int. Tech. Meeting Inst. Navigat.* Manassas, VA, USA: Institute of Navigation, Feb. 2019, pp. 233–247.
[28] C. Rieck, S. Gewies, L. Grundhöfer, and M. Hoppe, "Synchronization of R-mode base stations," in *Proc. Joint Conf. IEEE Int. Freq. Control Symp. Int. Symp. Appl. Ferroelectr. (IFCS-ISAF)*, Jul. 2020, pp. 1–5.

LARS GRUNDHÖFER (Graduate Student Member, IEEE) received the B.S. and M.S. degrees in electrical engineering from the Hamburg University of Technology, Harburg, Hamburg, Germany, in 2015 and 2017, respectively. He is currently working as a Scientist for the German Aerospace Center, Institute of Communications and Navigation. His current research interest includes terrestrial maritime navigation in the medium-frequency band.

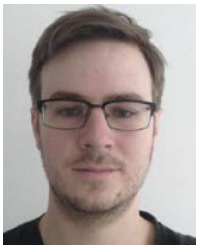

MARKUS WIRSING received the Master of Science degree in electrical engineering from Ulm University, Germany, in 2018. He is currently pursuing the Ph.D. degree with the German Aerospace Center (DLR), Institute of Communications and Navigation. In 2018, he joined the DLR, Institute of Communications and Navigation, as a Research Staff Member. His research interests include signal design and signal processing for maritime wireless communication and navigation systems.

STEFAN GEWIES received the Diploma degree in physics from Heidelberg University, in 2003, and the degree from Heidelberg University, in 2009, on the topic of modeling solid oxide fuel cells with Ni/YSZ cermet anodes.

He joined the German Aerospace Center, Institute of Communications and Navigation, in 2009, where he started working on GNSS applications and further development of the GNSS experimentation and verification networks (EVnets). He has led the Maritime Services Group, Nautical Systems Department, since 2015. His current research interest includes maritime terrestrial navigation systems.

GIOVANNI DEL GALDO (Member, IEEE) received the degree in telecommunications engineering from the Politecnico di Milano and the doctoral degree from Technische Universität Ilmenau, in 2007, on the topic of MIMO channel modeling for mobile communications.

He then joined the Fraunhofer Institute for Integrated Circuits IIS, working on audio watermarking and parametric representations of spatial sound. Since 2012, he has led a joint research group composed of a department at the Fraunhofer IIS and as a Full Professor and the Chair at Technische Universität Ilmenau (TU Ilmenau) on the research area of wireless distribution systems and digital broadcasting. Since 2016, the group has been merged with the Electronic Measurements Chair led by Prof. Reiner Thomä, giving birth to the Electronic Measurements and Signal Processing (EMS) Group. Since 2017, he has been the Director of the Institute for Information Technology, TU Ilmenau. He leads the VDE-ITG Expert Group HF.2 on Radio Systems. His current research interests include the analysis, modeling, and manipulation of multi-dimensional signals; over-the-air testing for terrestrial and satellite communication systems; and sparsity promoting reconstruction methods.